

# The Effect of Conductivity Values on Activation Times and Defibrillation Thresholds

Barbara M Johnston<sup>1</sup>, Josef P Barnes<sup>1</sup>, Peter R Johnston<sup>1</sup>

<sup>1</sup> Griffith University, Nathan, Queensland, Australia

## Abstract

*Uncertainty in the input parameters used in simulation studies needs to be taken into account when evaluating the results produced. This work considers the effect of using various sets of bidomain conductivity values in two simulations: firstly, activation times, which indicate the propagation of the depolarisation wavefront through the cardiac tissue, and, secondly, the determination of defibrillation thresholds in a ‘heart in a bath’ model, where a shock is delivered from two opposing patch electrodes. Both simulations use the same two types of sets of bidomain conductivity values: four-conductivity datasets (where normal and transverse conductivities are assumed equal) and six-conductivity datasets, including newly proposed sets that are based on experimental measurements.*

*The activation time maps show significant differences depending on the conductivity set used, as do the defibrillation thresholds. The defibrillation thresholds vary by more than 20%, whereas the activation times for epicardial breakthrough and total depolarisation both vary by approximately 50%. It is found that the most extreme values in each case are produced by two of the four-conductivity datasets. Since these differences are large enough to lead to different conclusions in such studies, it is suggested that the four-conductivity datasets may not be an appropriate choice for use in simulation studies in the heart.*

## 1. Introduction

Since electrophysiological simulations are used to increase understanding of aspects of cardiac electrophysiology that are not amenable to experimental study, it is worth considering the effect uncertainty in the input parameters may have on the results of such simulations. Studies that model the electric field in cardiac tissue, which consists of ‘sheets’ of cardiac fibres, normally use the bidomain model [1]. This continuum model regards tissue as consisting of two interpenetrating domains: intracellular ( $i$ ), the space within the cardiac cells, and extracellular ( $e$ ), the space outside the cells, but within the tissue. The two spaces

Table 1. Conductivity data (in  $\text{mS cm}^{-1}$ ) from the indicated studies. Dashes in the table indicate that the values do not exist. Here  $\alpha = g_{il}/g_{el}$ .

Study	$g_{el}$	$g_{et}$	$g_{en}$	$g_{il}$	$g_{it}$	$g_{in}$
Clerc [12]	6.3	2.4	–	1.7	0.19	–
Roberts et al. [13]	2.2	1.3	–	2.8	0.26	–
Roberts and Scher [14]	1.2	0.8	–	3.4	0.6	–
MacLachlan et al. [6]	2.0	1.7	1.4	3.0	1.0	0.32
Hooks et al. [5]	2.6	2.5	1.1	2.6	0.26	0.08
Johnston ( $\alpha = 1$ ) [10]	2.4	2.0	1.1	2.4	0.35	0.08
Johnston ( $\alpha = 0.6$ ) [10]	3.2	2.2	1.2	1.9	0.35	0.08
Johnston ( $\alpha = 1.6$ ) [10]	2.0	2.2	1.2	3.1	0.35	0.08

are separated everywhere by the cell membrane. The electric current is able to travel in three mutually orthogonal directions: longitudinal ( $l$ ); transverse ( $t$ ), and normal ( $n$ ), where the current is travelling along the cardiac fibres, perpendicular to the fibres within the sheet and perpendicular to the sheet, respectively. This results in six bidomain model conductivities,  $g_{pq}$  ( $p = i, e$  and  $q = l, t, n$ ).

Due to the considerable experimental and computational challenges associated with determining these conductivities [2], at present no experimentally determined sets of all six conductivities are available. More than thirty years ago, three sets of four conductivity values  $g_{pq}$  ( $p = i, e$  and  $q = l, t$ ) were found using different experimental setups and models (Table 1, rows 1–3). These values vary considerably, and to be used in modelling studies the assumption must be made that the normal conductivities are equal to the transverse conductivities. It has been shown that, in simulation studies modelling partial thickness ischaemia, these sets produce very different results from one another [3, 4] and from the two (non-experimental) six-conductivity datasets [5, 6] given in the literature (Table 1, rows 4 and 5) [7].

## 2. Sets of Bidomain Conductivity Values

In addition, recent experimental studies [8] have shown that cardiac tissue is orthotropic, contrary to the  $n = t$  assumption. The results of these studies, one of which [9] determined conduction velocities in each direction, and the

other [5], which determined bulk (intra– plus extracellular) conductivities, have been used [10] recently to propose new six conductivity datasets (Table 1, last three rows). These sets depend on the parameter  $\alpha = g_{il}/g_{el}$ , which is often taken to be 1. It is, however, not known and has been measured in the range 0.3–1.2 [11].

This paper considers the effect of using the various datasets described above (Table 1) in simulations that determine activation times and defibrillation voltages in models using a realistic canine geometry.

## 2.1. Normalised conductivities

Recently, it was shown [10] that it is possible to use the results of two experimental studies [5,9] to produce a set of normalised conductivity values. The studies showed that conduction velocities ( $c_q$ ,  $q = l, t, n$ ) divide approximately in the ratio  $c_l : c_t : c_n = 4 : 2 : 1$  [9] and so too do the bulk conductivities ( $g_q = g_{iq} + g_{eq}$ ,  $q = l, t, n$ ), that is,  $g_l : g_t : g_n = 4 : 2 : 1$  [5]. Assuming these are exact means that  $g_l/g_t = 2$  and  $c_l/c_t = \lambda_l/\lambda_t$ , and  $g_t/g_n = 2$  and  $c_t/c_n = \lambda_t/\lambda_n$  ( $\lambda_q$ =space constant), which implies that [10]

$$\frac{g_{il}g_{el}}{g_{it}g_{et}} = 8 \quad \text{and} \quad \frac{g_{it}g_{et}}{g_{in}g_{en}} = 8. \quad (1)$$

If the conductivities are then normalised with respect to  $g_{it}$  (indicated with a prime), for example  $g'_{et} = g_{et}/g_{it}$ , it is then possible to substitute in the above relationships for the bulk conductivities using equation (1) and determine a set of formulae [10] for the normalised conductivities, that depends only on  $\alpha = \frac{g_{il}}{g_{el}} = \frac{g'_{il}}{g'_{el}}$ . The set is, where  $\beta = \alpha + 1 + \sqrt{\alpha^2 + 1}$  and  $\gamma = \alpha + 1 + \sqrt{\alpha^2 + \alpha + 1}$ :

$$g'_{il} = 2\beta, g'_{el} = \frac{2\beta}{\alpha}, g'_{it} = 1, g'_{et} = \left(\frac{\alpha+1}{\alpha}\right)\beta - 1, \\ g'_{in} = \frac{\beta}{4\gamma}, g'_{en} = \frac{\beta\gamma}{4\alpha} \quad (2)$$

## 2.2. Six conductivity datasets

One suggested [10] approach to produce actual sets of conductivities from these normalised conductivities is to set  $g_{it} = 0.35$ , the average of the experimentally determined four–conductivity datasets (rows 1–3 in Table 1). In this case, setting  $\alpha$  across a wide range (here  $\alpha = 0.6, 1, 1.6$ ) leads to the six–conductivity datasets given in the last three rows of Table 1.

It would, of course, be possible to use other values to scale the normalised dataset. For example, another approach might be to start with the bulk conductivity values (in mS/cm) found by Hooks et al. [5] ( $g_l = 7, g_t = 3.5, g_n = 1.6$  mS/cm). If this is combined with the fact, shown in Johnston [10], that the various transverse to normal conductivity ratios are quite consistent across a

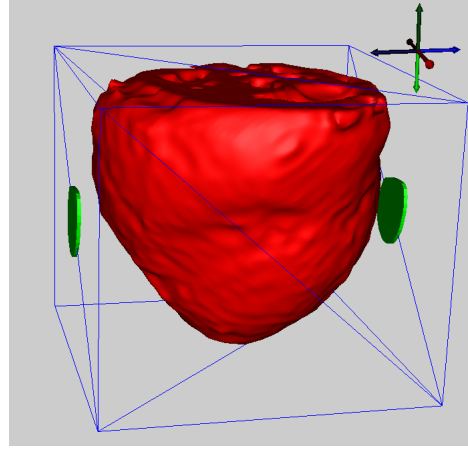


Figure 1. ‘Heart in a bath’ model, with blue lines for outside of bath, green discs for defibrillation paddles.

range of  $\alpha$  values (that is,  $g_{en}/g_{in} \approx 14$ ,  $g_{et}/g_{it} \approx 6$ ,  $g_{et}/g_{en} \approx 2$ ), then (for  $\alpha = 1$  and taking exact values for the ratios), the following dataset (in mS/cm) is obtained:  $g_{el} = 3.5, g_{et} = 3, g_{en} = 1.5, g_{il} = 3.5, g_{it} = 0.5, g_{in} = 0.11$ . However, a comparison of these values with those in Table 1 shows that these are higher than all but three of the values in the table, so this dataset will not be used.

## 3. Governing equations and models

Two versions of the bidomain equations [1] will be used in this work: the passive bidomain model (in the defibrillation model); and the active (transient) bidomain model, for producing activation time maps.

### Passive bidomain equations

$$\nabla \cdot \mathbf{M}_i \nabla \phi_i = \frac{\beta}{R_m} \phi_m \quad (3)$$

$$\nabla \cdot \mathbf{M}_e \nabla \phi_e = -\frac{\beta}{R_m} \phi_m \quad (4)$$

$$\therefore \nabla \cdot (\mathbf{M}_i + \mathbf{M}_e) \nabla \phi_e = -\nabla \cdot \mathbf{M}_i \nabla \phi_m \quad (5)$$

where  $\phi_a$  is the extracellular ( $a = e$ ) or intracellular ( $a = i$ ) potential in cardiac tissue,  $\phi_m = \phi_i - \phi_e$  is the transmembrane potential,  $\beta$  is the surface to volume ratio and  $R_m$  is the membrane resistance. Here  $\mathbf{M}_a(\mathbf{x})$  ( $a = i, e$ ) is a conductivity tensor, which allows for fibre rotation through the tissue [15].

### Active bidomain equation

Substituting  $\phi_i = \phi_m + \phi_e$  in equation (3), and including a time–varying transmembrane current, gives

$$\nabla \cdot \mathbf{M}_i \nabla \phi_e + \nabla \cdot \mathbf{M}_i \nabla \phi_m = \beta \left( C_m \frac{\partial \phi_m}{\partial t} + I_{ion} \right) \quad (6)$$

where  $t$  is time,  $C_m$  is the membrane capacitance and  $I_{\text{ion}}$  is the ionic current density, determined, in this study, by the ten Tusscher and Panfilov [16] cell model.

### 3.1. A simple defibrillation model

A simple model for defibrillation of the heart can be created by considering a heart situated in a fluid bath with electrode paddles attached to opposite sides of the bath, as shown in Figure 1. The heart has a realistic canine geometry, obtained from MRI data, and includes realistic fibre orientation taken from diffusion weighted images [17]. The bath and ventricles are filled with a fluid having the same electrical properties as blood.

Equation (5), along with Laplace’s equation for the potential in the blood  $\phi_b$ ,

$$\nabla^2 \phi_b = 0 \quad (7)$$

is solved using the finite element method as implemented in SCIRun [17], with an additional mass matrix module developed by P. Johnston. The mesh contains 139,403 nodes joined by 820,244 tetrahedral elements. The boundary conditions are: that the outside of the bath, apart from the electrodes, is insulated, and there is continuity of potential and current, in the extracellular space, between the tissue and the bath. The two electrodes are set at fixed potentials, one of which is zero.

The various six-conductivity sets used in Sections 3.1 and 3.2 are given in Table 1. For the four-conductivity datasets it is assumed that the normal and transverse conductivities are equal. The parameters used to solve equations (5) and/or (6) are:  $g_b = 6.7 \text{ mS/cm}$ ,  $\beta = 2000 \text{ cm}^{-1}$ ,  $R_m = 9100 \Omega \text{ cm}^2$  and  $C_m = 2 \mu \text{ F/cm}^2$ .

### 3.2. Activation time maps

The heart geometry for these simulations is the same as that described in the previous section, with the ventricles full of blood, except that the heart is isolated rather than being in a bath. The boundary conditions are similar to those in the previous section, except the epicardium is insulated and a stimulating current is applied at the apex of the endocardium at time  $t = 0$ . The model is solved using the finite volume method on a mesh with 717,709 nodes connected by 4,486,917 tetrahedral elements [15]. From this activation time maps (see Figure 2) were produced.

## 4. Results and discussion

### 4.1. Activation times

Firstly, two different types of activation times were produced using the model (Section 3.2) along with the eight

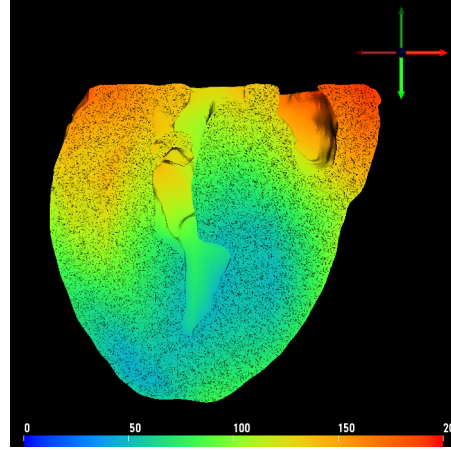


Figure 2. Cross-section of the heart, showing an activation time map produced using Clerc’s data.

sets of conductivities listed in Table 1 and using the above parameters. They were: the time to surface breakthrough, and the time to complete depolarisation. The results in Table 2 (columns 2 and 3) show that the activation times depend on the conductivity set used in the simulation. As would be expected, there is a strong correlation ( $r^2=0.99$ ) between the time to surface breakthrough and the time to complete depolarisation. For both types of activation time there is approximately a 50% difference between the quickest and slowest times: 30 and 46 ms for surface breakthrough and 126 and 197 ms for total depolarisation. In this case MacLachlan [6] and Roberts and Scher [14] are equally quick and Clerc [12] is the slowest. The remaining results vary by less than 20%.

### 4.2. Defibrillation voltages

Next, the ‘heart in a bath’ model (Section 3.1) was run using the same conductivity sets and parameters. Increasing potential differences were applied across the paddles (Figure 1) until the threshold potential difference was found that met the defibrillation target of at least 90% of the extracellular tissue having a potential gradient of 6 V/cm.

The results are given in Table 2 (column 4) and again depend on the conductivity set used. In addition to there being an approximately 20% difference between the lowest (173 V) and highest threshold values (209 V), it can also be seen that the lowest and highest values are produced by four-conductivity datasets, that is, those of Roberts and Scher [14] and Clerc [12], respectively. The voltages for the remaining datasets lie within 5% of one another.

Table 2. Activation times (in ms) and threshold potential differences (in V), for various conductivity datasets.

Dataset	Time to Surface Break-through (ms)	Time to Complete Depolarisation (ms)	Defibrillation Threshold Potential Difference (V)
MacLachlan	30	127	179
Roberts&Scher	31	126	173
Roberts et al.	37	153	180
Hooks	38	165	190
Johnston( $\alpha = 1$ )	39	169	184
Johnston( $\alpha = 1.6$ )	43	188	186
Johnston( $\alpha = 0.6$ )	44	188	188
Clerc	46	197	209

## 5. Conclusion

This work has demonstrated that, when simulations are carried out using the bidomain equations to model the electric potential in cardiac ventricular tissue, both activation times and defibrillation voltages are significantly affected by the conductivity values that are used. Although the simulations presented here use a realistic heart geometry, both models are simplified in that one is a simple ‘heart in a bath’ and the other is lacking the Purkinje system, resulting in slower activation times. However, these are not significant limitations as the purpose of this study is to compare the effect of the input conductivities. The effect is particularly noticeable for the four-conductivity datasets (Table 1, rows 1–3), as well as that of MacLachlan et al. [6]. Hence, it is suggested that researchers should use one of the six-conductivity datasets from Table 1 (rows 5–8) in cardiac electrophysiological simulations that use the bidomain model.

## References

- [1] Tung L. A Bi-domain model for describing ischaemic myocardial D-C potentials. Ph.D. thesis, Massachusetts Institute of Technology, June 1978.
- [2] Clayton RH, Bernus O, Cherry EM, Dierckx H, Fenton FH, Mirabella L, Panfilov AV, Sachse FB, Seemann G, Zhang H. Models of cardiac tissue electrophysiology: Progress, challenges and open questions. *Progress in Biophysics and Molecular Biology* 2011;104(1–3):22–48.
- [3] Johnston PR, Kilpatrick D. The effect of conductivity values on ST segment shift in subendocardial ischaemia. *IEEE Transactions on Biomedical Engineering* February 2003; 50(2):150–158.
- [4] Johnston PR. A sensitivity study of conductivity values in the passive bidomain equation. *Mathematical Biosciences* 2011;232(2):142–150.
- [5] Hooks D. Myocardial segment-specific model generation for simulating the electrical action of the heart. *BioMedical Engineering OnLine* 2007;6(1):21–21.
- [6] MacLachlan MC, Sundnes J, Lines GT. Simulation of ST segment changes during subendocardial ischemia using a realistic 3-D cardiac geometry. *IEEE Transactions on Biomedical Engineering* 2005;52(5):799–807.
- [7] Johnston BM, Johnston PR. The sensitivity of the passive bidomain equation to variations in six conductivity values. In Boccaccini A (ed.), *Proceedings of the 10th IASTED International Conference Biomedical Engineering (BioMed 2013)*. IASTED, Calgary, Alberta, Canada: ACTA Press, February 2013; 538–545.
- [8] Hooks DA, Trew ML, Caldwell BJ, Sands GB, LeGrice IJ, Smaill BH. Laminar arrangement of ventricular myocytes influences electrical behavior of the heart. *Circulation Research* 11 2007;101(10):e103–112–e103–112.
- [9] Caldwell BJ, Trew ML, Sands GB, Hooks DA, LeGrice IJ, Smaill BH. Three distinct directions of intramural activation reveal nonuniform side-to-side electrical coupling of ventricular myocytes. *Circulation Arrhythmia and Electropysiology* 2009;2:433–440.
- [10] Johnston BM. Six conductivity values to use in the bidomain model of cardiac tissue. *IEEE Transactions on Biomedical Engineering* 2016;63(7):1525–1531.
- [11] Roth BJ. Electrical conductivity values used with the bidomain model of cardiac tissue. *IEEE Transactions on Biomedical Engineering* April 1997;44(4):326–328.
- [12] Clerc L. Directional differences of impulse spread in trabecular muscle from mammalian heart. *Journal of Physiology* 1976;255:335–346.
- [13] Roberts DE, Hersh LT, Scher AM. Influence of cardiac fiber orientation on wavefront voltage, conduction velocity and tissue resistivity in the dog. *Circulation Research* 1979; 44:701–712.
- [14] Roberts DE, Scher AM. Effects of tissue anisotropy on extracellular potential fields in canine myocardium in situ. *Circulation Research* 1982;50:342–351.
- [15] Barnes JP. Mathematically modeling the electrophysiological effects of ischaemia in the heart. Ph.D. thesis, Griffith University, Brisbane, Australia, 2013.
- [16] ten Tusscher KHWJ, Panfilov AV. Alternans and spiral breakup in a human ventricular tissue model. *American Journal of Physiology Heart and Circulatory Physiology* 2006;291(3):H1088–H1100.
- [17] URL <http://www.scirun.org>. SCIRun: A Scientific Computing Problem Solving Environment, Scientific Computing and Imaging Institute (SCI).

Address for correspondence:

Barbara Johnston  
 School of Natural Sciences and Queensland Micro- and Nanotechnology Centre, Griffith University, Kessels Rd, Nathan, Queensland, Australia  
 Barbara.Johnston@griffith.edu.au